Interaction of Fluorescence Labeled Single-Stranded DNA with Hexameric DNA-Helicase RepA: A Photon and Fluorescence Correlation Spectroscopy Study†

Hai Xu,‡ Joachim Frank,*,§ Ulrike Trier,|| Stefanie Hammer,|| Werner Schröder,‡ Joachim Behlke,⊥ Monika Schäfer-Korting,|| Josef F. Holzwarth,§ and Wolfram Saenger‡

Institut für Kristallographie, Freie Universität Berlin, Takustrasse 6, D-14195 Berlin, Germany, Fritz-Haber-Institut der Max-Planck-Gesellschaft, Faradayweg 4-6, D-14195 Berlin, Germany, Institut für Pharmazie II, Abteilung für Pharmakologie und Toxikologie, Freie Universität Berlin, Königin-Luise-Strasse 2-4, D-14195 Berlin, Germany, and Max-Delbrück-Zentrum für Molekulare Medizin, Robert-Rössle-Strasse 10, D-13122 Berlin, Germany

Received July 5, 2000; Revised Manuscript Received April 12, 2001

ABSTRACT: Fluorescence correlation spectroscopy (FCS) was used to characterize the interaction of fluorescence labeled single-stranded DNA (ssDNA) with hexameric RepA DNA-helicase (hRepA) encoded by plasmid RSF1010. The apparent dissociation constants, $K_{d(app)}$, for the equilibrium binding of 12mer, 30mer, and 45mer ssDNA 5′-labeled with BFL to hRepA dimer in the presence of 0.5 mM ATPγS at pH 5.8 and 25 °C were determined to be 0.58 ± 0.12, 0.52 ± 0.07, and 1.66 ± 0.32 μM, respectively. Binding curves are compatible with one binding site for ssDNA present on hRepA dimer, with no indication of cooperativity. At pH 7.6 in the presence of ATPγS and at pH 5.8 in the absence of ATPγS, complex formation between ssDNA and hRepA was too weak for measuring complete binding curves by FCS. Under these conditions, the dissociation constant, $K_{d(app)}$, is in the range between 10 and 250 μM. The kinetics of complex formation at pH 5.8 are faster than the time resolution (approximately 10−20 s) of FCS experiments under pseudo-first-order conditions, with respect to BFL-ssDNA. Photon correlation spectroscopy (PCS) experiments yielded, within the experimental error range, the same values for the apparent hydrodynamic radii, R_h, of hRepA dimer and its complex with ssDNA as determined by FCS (R_h = 6.6 ± 1 nm). hRepA starts to aggregate under acidic conditions (<pH 6.0) which are optimal for ssDNA binding. CD spectra taken at pH 5.8 in the presence of ATPγS showed a structural change induced by ssDNA binding to hRepA which is not visible at pH 7.6 and with ADP as nucleotide cofactor.

DNA helicases are motor proteins involved in key biological processes such as DNA replication, repair, recombination, transcription, and translation. They are fueled by nucleoside 5′-triphosphates (NTPs) and catalyze the strictly processive unwinding of double-stranded DNA (dsDNA)[1] either in the 5′→3′ or in the 3′→5′ direction (*1*). All DNA helicases for which the assembly state of the enzyme has been examined appear to function as oligomers, generally dimers or hexamers, thus providing multiple potential DNA binding sites, which are required for helicase function. The *E. coli* DnaB protein (*2*), the bacteriophage T7 gp4 protein (*3*), the *E. coli* transcription termination protein Rho (*4*), and plasmid RSF1010 encoded hexameric RepA helicase (hRepA) assemble as hexamers into a ring-shaped structure (*5*). These helicases have in common a central channel through which single-stranded DNA is assumed to pass (*6*−*8*).

hRepA is one of the smallest known DNA helicases with a molecular mass of 6 × 29.896 kDa (*5*). In contrast to other multimeric helicases that require Mg^{2+}, ATP, or ssDNA to assemble into an enzymatically active form, the hexameric structure of hRepA is stable even in the absence of any cofactor. The optimum helicase activity is at slightly acidic conditions around pH 5.6−6.0, a property that is shared only by DNA-helicases from *Saccharomyces cerevisiae* (*9*). hRepA assembles into tubular aggregates below pH 6.0 (*10*), and the three-dimensional structure determined by X-ray diffraction methods was refined to 2.4 Å resolution (*11*). hRepA is pot-shaped with outer dimensions of 110 Å diameter and 60 Å height, and a central hole with 17 Å diameter. The six RepA monomers are identical to each other, and model building studies suggest that ATP is wedged into clefts between monomers, with the triphosphate moieties located in Walker A motifs typical of ATP-hydrolyzing enzymes. In the crystals, hRepA are orientated back-to-back to form dimers of hRepA hexamers (dodecamers) stabilized

† These studies were supported by the Deutsche Forschungsgemeinschaft, Fonds der Chemischen Industrie, and an EU-Project on helicases.

* Corresponding author. Phone: +49-30-8413-5517, FAX: +49-30-8413-3155, E-mail: frank_j@fhi-berlin.mpg.de.

‡ Institut für Kristallographie, Freie Universität Berlin.

§ Fritz-Haber-Institut der Max-Planck-Gesellschaft.

|| Institut für Pharmazie II, Freie Universität Berlin.

⊥ Max-Delbrück-Zentrum für Molekulare Medizin.

[1] Abbreviations: BODIPY FL, 4,4-difluoro-5,7-dimethyl-4-bora-3*a*,4*a*-diaza-*s*-indacene-3-propionic acid; BFL, BODIPY FL; ssDNA, single-stranded oligodeoxynucleotide; dsDNA, double-stranded oligodeoxynucleotide; BFL-ssDNA, phosphoramidate adduct of BFL and ssDNA; MES, 2-(*N*-morpholino)ethanesulfonic acid; ATPγS, adenosine 5′-*O*-(3-thiotriphosphate); TMR, tetramethylrhodamine; TMR-maleimide, tetramethylrhodamine-maleimide; TMR-hRepA, tetramethylrhodamine-labeled hRepA; hRepA, hexameric RepA; DTT, dithiothreitol; EDTA, ethylenediaminetetraacetic acid; EDAC, ethyl[(dimethylamino)propyl]carbodiimide; FCS, fluorescence correlation spectroscopy; PCS, photon correlation spectroscopy; ITC, isothermal titration calorimetry; CD, circular dicroism.

10.1021/bi001543o CCC: $20.00
Published on Web 05/25/2001

by direct protein−protein contacts. The dimers are stacked like coins in a roll, giving rise to cylinders reminiscent of the tubular structures mentioned above that form at pH <6.0. The position of ATP between RepA monomers explains the cooperativity of binding of ATP and the nonhydrolyzable analogue ATPγS to hRepA, with Hill coefficients around 2.0 (*12*). The helicase reaction is maximal between pH 5.5 and 6.0 at low salt concentration ([NaCl] ≤20 mM), although at these conditions aggregation occurs (*10*). Salt at higher concentrations inhibits the helicase reaction (*5*). In the presence of 60 mM NaCl at pH 5.8, hRepA dimer with no indication of aggregates was identified in analytical ultracentrifugation experiments (*13*). Since the unwinding reactions require 5′-tailed ssDNA for hRepA helicase to translocate, and hydrolysis of ATP is stimulated by the presence of ssDNA, it was of interest to further investigate the binding of different lengths of ssDNA oligomers to hRepA at maximum helicase activity condition (pH 5.8 without NaCl) and also the influence of nucleotide cofactors on binding, which is the topic of this study. For the determination of dissociation constants, we measured the degree of saturation for the binding of ssDNA 5′-labeled with BODIPY FL to hRepA, using fluorescence correlation spectroscopy (FCS).

During an FCS experiment, a sharply focused laser beam passes through a very small volume element (0.2×10^{-15} to 1×10^{-15} L) of the sample under study. At any given time, there are only a few (1−5) fluorescent particles in this volume. Since the particles undergo Brownian motion in solution, the resulting time-dependent fluctuation of the fluorescence signal can be analyzed in terms of an autocorrelation function, yielding translational diffusion times (τ_{diff}) for the fluorescent species present. The relative fraction of each species can be obtained from the autocorrelation function, provided that their molecular masses differ by at least 1:7 and their diffusion times by a factor of 1.6 (*14*, *15*). The apparent hydrodynamic radii (R_h) and the diffusion coefficient (D) of hRepA and its complexes with ssDNA of different lengths and the binding affinities were determined. To compare the results derived by FCS, additional dynamic light scattering (photon correlation spectroscopy, PCS) experiments were carried out.

EXPERIMENTAL PROCEDURES

All salts and buffer components were from Merck (Darmstadt, Germany). They were of p.a. quality and used without further purification. BODIPY FL (4,4-difluoro-5,7-dimethyl-4-bora-3*a*,4*a*-diaza-*s*-indacene-3-propionic acid; D-2183), hereafter called BFL, and the FluoReporter Oligonucleotide Phosphate Labeling Kit (F-6096) for labeling of 5′-phosphate-terminated oligodeoxynucleotides with a BFL derivative were from Molecular Probes Europe (Leiden, The Netherlands). ssDNA was purchased from TIB MOLBIOL (Berlin, Germany).

One hundred micrograms of ssDNA was phosphorylated at the 5′-terminus with 100 units of T4 polynucleotide kinase (New England BioLabs GmbH, Frankfurt, Germany) in a total volume of 100 μL containing 2.5 mM ATP, 10 mM $MgCl_2$, 5 mM DTT, 0.1 mM spermidine, 0.1 mM EDTA, and 50 mM Tris-HCl buffer, pH 7.6. The reaction mixture was incubated for 2 h at 37 °C followed by precipitation of the resulting 5′-phosphate-terminated ssDNA by ethanol. The 5′-phosphate-terminated ssDNA was then dissolved in a volume of 10 μL at a concentration of 10 μg/μL.

According to the protocol supplied by Molecular Probes Europe, 10 μL of the 5′-phosphate-terminated oligodeoxynucleotide stock solution (10 μg/μL) was added to 20 μL of H_2O, 50 μL of labeling buffer (0.24 M methylimidazole, pH 9.0, 0.32 M EDAC), and 20 μL (10 μg/μL) of the phosphate-reactive cadaverine derivative of BFL dissolved in DMSO. The reaction mixture was placed on a shaker oscillating at low speed and allowed to react for 4 h at room temperature, resulting in a reasonably stable phosphoramidate adduct. Finally the fluorescence labeled BFL-ssDNAs were precipitated with ethanol. The precipitates were dissolved in 50 mM triethylammonium acetate, pH 7.0, and applied to reversed-phase HPLC using a C18 column with a linear 5−60% acetonitrile/water gradient over 120 min to separate unlabeled ssDNA, labeled ssDNA, and free dye (*16*).

Helicase hRepA was purified from *Escherichia coli* as described by Röleke et al. (*10*). For control experiments, hRepA was directly labeled at the only cysteine in the sequence (Cys 172) with TMR-maleimide (T-6027) from Molecular Probes Europe (Leiden, The Netherlands). To a 100 μL solution of hRepA (15 mg/mL) containing 20 mM Tris-HCl, pH 8.0, 0.1 mM EDTA, and 150 mM NaCl was added a 10 μL aliquot of a 10 mM stock solution of TMR-maleimide dissolved in DMSO (TMR-maleimide:hRepA molar ratio = 12). The reaction was terminated after 1 h by the addition of a 10-fold excess of *N*-acetylcysteine with respect to TMR-maleimide. Labeled hRepA was passed through a PD20 column (Pharmacia) followed by extensive dialysis against 20 mM Tris-HCl, pH 8.0, to remove unreacted dye. The stoichiometry of the labeled product was 1.2 TMR/hRepA hexamer as determined by UV−Vis spectrometry.

For investigating the interaction of ssDNA with hRepA, two different buffers (A and B) were used. They consist of (A) 40 mM MES−NaOH, 10 mM $MgCl_2$, pH 5.8, and (B) 40 mM Tris-HCl, 10 mM $MgCl_2$, pH 7.6. FCS measurements were conducted with hRepA in the presence of ATPγS, $MgCl_2$, and BFL-d$(A)_{12}$, BFL-$(A)_{30}$, or BFL-45mer ssDNA with the nucleotide sequence 5′-ACTCTAGAGGATC-CCCGGGTACGTTATTGCATGAAAGCCCGGCTG-3′.

The following possible partial duplex structure of 45mer ssDNA will be considered under Discussion:

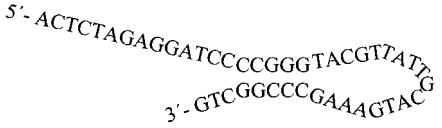

Fluorescence Correlation Spectroscopy (FCS). (A) Theoretical Considerations. In this paper, we will only give a very basic introduction to FCS, mainly based on user information distributed by EVOTEC GmbH, Hamburg (*17*). A detailed description of the underlying theory and possible experimental applications may be found elsewhere (*14*, *15*, *18*−*24*). For a reversible bimolecular reaction of a labeled small ligand (A*) and a macromolecule (B):

$$A^* + B \Leftrightarrow A^*B$$

the autocorrelation function, $G(\tau)$, can be expressed in terms of a two-component model (*25*). Since the solution also

contains free dye which could not be completely removed by HPLC, it is necessary to apply a three-component model according to eq 1 (Dr. Hecks, EVOTEC GmbH, personal communication). The autocorrelation curves were evaluated with a Marquardt nonlinear least-squares fitting routine, as implemented in the program FCS Access 2.0 (EVOTEC GmbH). The following three-component model corresponding to free BFL, free BFL-ssDNA, and the complex between BFL-ssDNA and hRepA was used:

$$G(\tau) = \left[1 - P + P\exp\left(\frac{-\tau}{\tau_P}\right)\right]N^{-1} \times \left[\frac{1-y-z}{\left(1+\frac{\tau}{\tau_1}\right)\sqrt{1+\frac{r_0^2}{z_0^2}\frac{\tau}{\tau_1}}} + \frac{y}{\left(1+\frac{\tau}{\tau_2}\right)\sqrt{1+\frac{r_0^2}{z_0^2}\frac{\tau}{\tau_2}}} + \frac{z}{\left(1+\frac{\tau}{\tau_3}\right)\sqrt{1+\frac{r_0^2}{z_0^2}\frac{\tau}{\tau_3}}}\right] \quad (1)$$

with

$$z = \frac{[A^*B]}{[A^*] + [A^*B]}$$

In this equation, P is the average fraction of dye molecules in the triplet state with relaxation time τ_P, N is the total average number of fluorescent molecules in the observation volume, y and z are the relative concentration fractions of free and bound A*, respectively, τ_1, τ_2, and τ_3 define the average time (diffusion time) for detected molecules of free dye, free A*, and bound A*, respectively, and r_0 and z_0 are the lateral and axial distances, respectively, between the positions where the Gaussian emission light distribution adopts the maximum value and the point where the light intensity decreases to $1/e^2$ of the maximum value (this defines the observation volume). Lateral and axial lengths of the observation volume are related through the structure parameter SP:

$$z_0 = \mathrm{SP} r_0 \quad (2)$$

To obtain r_0, the translational diffusion time, τ_{diff}, of a standard (Rhodamine 6G) is measured. The diffusion time is related to r_0 through

$$\tau_{diff} = \frac{r_0^2}{4D} \quad (3)$$

where D is the translational diffusion coefficient of the standard. From the experimentally determined diffusion coefficient, an apparent hydrodynamic radius, R_h, can be calculated according to the Stokes−Einstein equation:

$$R_h = \frac{kT}{6\pi\eta D} \quad (4)$$

were k is the Boltzmann constant, T the absolute temperature, and η the viscosity of the solution; at low concentration of solute and buffer, the solvent viscosity can be used.

(B) Experimental Setup. FCS measurements were performed with a ConfoCor I fluorescence correlation spectrometer (Carl Zeiss Jena GmbH, Jena, Germany; EVOTEC Biosystems GmbH, Hamburg, Germany). The samples were excited using an argon laser at a wavelength of 488 nm for BFL adducts. Fluorescence emission was detected between 520 and 570 nm. The fluorescence of TMR-labeled hRepA was excited at 514 nm with the same laser, and emission was detected between 520 and 610 nm.

For the determination of binding constants, solutions of 15 nM BFL-ssDNA were incubated in buffer A or B with an excess of hRepA (between 0.02 and 50 μM) at room temperature for at least 15 min. Then 100 μL of the sample solution was filled into a chambered coverglass (Lab-Tec, NUNC GmbH, Wiesbaden, Germany), which was placed directly above the objective (C-Apochromat 40×/1.2 water immersion) through which the laser beam passed. The same objective served to collect the fluorescence emission. Spectra were sampled for 45 s if not otherwise indicated. Each single measurement was repeated 10 times, and the results were averaged. The autocorrelation functions of the intensity fluctuations were automatically recorded on 288 channels which were quasi-logarithmically spaced in time. These channels cover the dynamic range between 200 ns and 3438 s. Note that a strict temperature control is usually not required, because small fluctuations induced by moderate temperature changes can be neglected (*19*).

Prior to the experiments, the structure parameter SP (see eqs 2 and 3) was determined with a standard Rhodamine 6G solution. For the diffusion coefficient of Rhodamine 6G, a value of 2.8×10^{-10} m^2 s^{-1} was used (*23*). The translational diffusion time constants of free BFL, free BFL-ssDNA, and the BFL-ssDNA/hRepA complex were measured in independent experiments and served as input parameters for further fitting procedures. According to eq 1, the relative concentration fractions of free, y, and bound BFL-ssDNA, z, the fraction of fluorescent molecules in the triplet state, P, the diffusion time of triplet states, τ_P, and the total number of fluorescent species, N, served as variable parameters. The fraction of triplet states of BFL-labeled ssDNA and its complex with hRepA was between 10 and 20% for all experiments. This low triplet yield did not influence the accuracy of data evaluation according to eq 1.

Photon Correlation Spectroscopy (PCS). (A) Theoretical Considerations. The theory of light scattering has been reviewed in several monographs (*26*−*28*), so we give only a very basic introduction to the method.

In a typical light scattering experiment, a laser beam impinges on a solution, and the scattered light is recorded by a photomultiplier. The spatial resolution of the experiment is defined by the scattering vector **q** whose magnitude is given by the Bragg formula:

$$|\mathbf{q}| = \frac{4\pi n}{\lambda}\sin\left(\frac{\theta}{2}\right) \quad (5)$$

Here λ denotes the wavelength of the scattered light, n the refractive index of the solution, and θ the scattering angle.

In a PCS experiment, the fluctuations of the scattered light due to the Brownian motion of the particles are analyzed in terms of the autocorrelation function (ACF), $G^{(1)}(\tau)$, which is proportional to the distribution of relaxation times, τ_{rel}, and scattering amplitudes of the examined components:

$$G^{(1)}(\tau) \propto \int_{R_{min}}^{R_{max}} N(R)M^2(R)P(q)S(q) \times \exp(-mR^{-1}q^2\tau_{rel})\, dR \quad (6)$$

Here m is a proportionality constant, $N(R)$ and $M(R)$ denote the number and mass, respectively, of particles with radius R between the integration limits R_{min} and R_{max}, and $P(q)$ and $S(q)$ denote the form and static structure factors, respectively, of the particles. If the particles are noninteracting and small compared with the employed wavelength, the translational diffusion coefficient, D, can be determined through Laplace inversion of the ACF. From D, the apparent hydrodynamic radii, R_h, of the particles are calculated according to the Stokes−Einstein equation (eq 4).

(B) Experimental Setup. PCS experiments were performed using a light scattering facility (Dierks and Partner, Hamburg, Germany). Measurements were performed at a scattering angle of 90°. A 50 mW diode laser (687 nm) served as light source. Intensity ACFs were automatically accumulated for 20 s in the relaxation time range between 1 μs and 10 s. Under these conditions, particles in the size range between 2 nm and 1 μm can be detected simultaneously. ACF spectra were Laplace-inverted by CONTIN (*29*, *30*), which is implemented in the facility used. For light scattering experiments, the samples were diluted with 40 mM Tris-HCl buffer of pH 7.6 (6.5) or 40 mM MES−NaOH buffer of pH 5.8 to a final concentration of 0.15 mg/mL. To remove dust, all samples were filtered before each measurement through sterile filters (Minisart; Sartorius, Göttingen, Germany) of 200 or 800 nm pore size.

Isothermal Titration Calorimetry (ITC). ITC experiments of ssDNA binding to hRepA were performed in MES−NaOH buffer of pH 5.8 (0.5 mM ATPγS and 10 mM $MgCl_2$) using an OMEGA high-sensitive microcalorimeter (MicroCal, Inc., Northampton, MA). A detailed description of the design and operation of this instrument has been provided previously (*31*). For measurements of the heat production accompanying the binding of ssDNA to hRepA, the enzyme was loaded into the sample cell of the calorimeter (volume = 1.3592 mL) at a concentration of 1.68 mg/mL (9.4 μM), and the reference cell was filled with distilled water or buffer, accordingly. Solutions of 1 mM $d(A)_{12}$ were filled into 100 μL syringes. The system was allowed to equilibrate until a stable baseline was observed before an automated titration was initiated. A typical experiment involved 25 injections of 3 μL of ssDNA solution into the sample cell at time intervals of 3 min. Throughout the titration, the cell was stirred continuously at 400 rpm. The molar enthalpy change for the binding of $d(A)_{12}$ to RepA, ΔH_b, was evaluated by integration of the whole heat production curves for 25 injections of $d(A)_{12}$ in a solution of 1.68 mg/mL hRepA. From the resulting enthalpy change ΔH, we subtracted the heat of dilution for the injection of $d(A)_{12}$ in MES−NaOH buffer, pH 5.8, without hRepA.

Circular Dichroism Spectroscopy. CD spectra between 195 and 250 nm were recorded using a Jasco J-600 spectropolarimeter coupled to an IBM-compatible microcomputer. All experiments were conducted using a cell with an optical path length of 1 mm. A scan speed of 20 nm/min and a step size of 0.2 nm were used throughout. Temperature was kept constant at 25 °C by a Lauda RC6 thermostat; five runs were averaged for the final spectra. The hRepA concentration was 0.3 mg/mL (1.7 μM) in 40 mM Tris-HCl buffer at pH 7.6 or in 40 mM MES−NaOH buffer at pH 5.8.

RESULTS

Fluorescence Correlation Spectroscopy (FCS) Studies. (A) Characterization of the Complex between BFL-Labeled DNA and hRepA. Figure 1 shows typical autocorrelation functions for BFL, BFL-$d(A)_{30}$, and BFL-$d(A)_{30}$/hRepA, respectively. The autocorrelation functions are consistent with the increasing molar mass of the solutes. From the autocorrelation functions, only three components can be reliably determined. Since in every experiment free BFL is present which diminishes the signal-to-noise ratio, it is essential to reduce the amount of free BFL to a minimum. For the detection of different fluorescent species, a mass difference of at least 1:7 or differing diffusion times by at least a factor of 1.6 are required (*14*, *15*). Therefore, mono-, bi-, and multiliganded hRepA molecules cannot be distinguished by the evaluation of the autocorrelation functions according to eq 1 and are observed as one fluorescent species. The diffusion coefficients (D) and the apparent hydrodynamic radii (R_h) for free BFL, BFL-labeled ssDNA of variable lengths, and the complexes between labeled ssDNA and hRepA were calculated according to eqs 3 and 4, and are given in Table

Table 1: Translational Diffusion Times (τ_{diff}), Diffusion Coefficients (D), and Apparent Hydrodynamic Radii (R_h) for All Investigated Species As Determined by FCS[a]

	τ_{diff} (ms)	D (m^2/s)	R_h (nm)	MW (×1000)
BFL	0.056 ± 0.001	(2.9 ± 0.1) × 10^{-10}	0.74 ± 0.03	0.292
BFL-$d(A)_{12}$	0.198 ± 0.009	(8.3 ± 0.5) × 10^{-11}	−	3.977
BFL-$d(A)_{30}$	0.23 ± 0.02	(7.2 ± 0.7) × 10^{-11}	−	9.597
BFL-45mer ssDNA	0.26 ± 0.03	(6.3 ± 0.7) × 10^{-11}	−	14.11
BFL-$d(A)_{12}$/hRepA	0.56 ± 0.06	(2.9 ± 0.3) × 10^{-11}	7.4 ± 0.8	∼360
BFL-$d(A)_{30}$/hRepA	0.59 ± 0.05	(2.8 ± 0.3) × 10^{-11}	7.8 ± 0.9	∼360
BFL-45mer ssDNA/hRepA	0.54 ± 0.08	(3.1 ± 0.5) × 10^{-11}	7.1 ± 1.1	∼360
TMR-hRepA	0.32 ± 0.03	(5.1 ± 0.5) × 10^{-11}	4.3 ± 0.4	179.4

[a] For comparison, the corresponding molecular weights (MW) are displayed. The diffusion coefficients (D) and apparent hydrodynamic radii (R_h) were calculated from the measured diffusion times, τ_{diff}, according to eqs 3 and 4. Experimental conditions: 40 mM MES−NaOH, pH 5.8 (10 mM $MgCl_2$, 0.5 mM ATPγS), 298 K. The confocal volume was 3.45 × 10^{-16} L. For the diffusion time of Rhodamine 6G, a value of 0.059 ms was determined; therefore, the structure parameter is 6.48. Due to limitations of the FCS technique, the concentration of the fluorescent BFL-ssDNAs could not be increased over 15 nM. Therefore, a 2000-fold excess of hRepA (40 μM) over BFL-ssDNA (15 nM) was used to saturate hRepA for determining the translational diffusion times of the complexes. The translational diffusion time of TMR-hRepA was measured with 20 mM Tris-HCl, pH 8.0, as buffer. (−) The hydrodynamic radius, R_h, of elongated ssDNA cannot be calculated according to eq 4 because this equation is only valid for globular macromolecules.

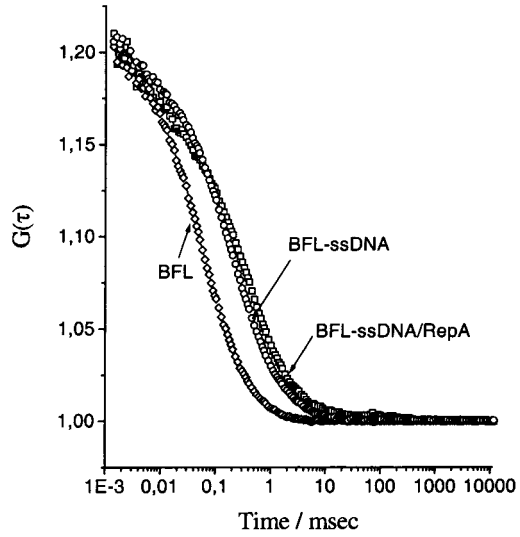

FIGURE 1: Fluorescence autocorrelation functions, $G(\tau)$, as a function of the channel time for the translational diffusion of BFL (5 nM), BFL-d(A)$_{30}$ (15 nM), and hRepA (40 μM) in complex with BFL-d(A)$_{30}$ (15 nM). All experiments were performed in 40 mM MES−NaOH (10 mM $MgCl_2$, 0.5 mM ATPγS) at pH 5.8 and 25 °C. The confocal volume was 3.5×10^{-16} L.

1. The diffusion times τ_{diff} of the fluorescence labeled single-stranded oligodeoxynucleotides increase with their molecular weight (Table 1). For each BFL-ssDNA, τ_{diff} is identical within the experimental error range at pH 5.8 and pH 7.6 (data not shown). The values of the diffusion times of the complexes between hRepA and BFL-d(A)$_{12}$, BFL-d(A)$_{30}$, and BFL-45mer ssDNA are nearly the same (0.56 ± 0.06 ms), but they are significantly longer than the value of τ_{diff} for TMR-labeled hRepA (0.32 ± 0.03 ms) which was measured in the absence of ssDNA at pH 8.0 (Table 1). For the measured diffusion times τ_{diff} of the ssDNA/hRepA complexes, D and R_h were calculated according to eqs 3 and 4 (Table 1). The radius, R, of a globular protein with a molecular weight, MW, is given by

$$R = \sqrt[3]{\frac{3MW}{4\pi\rho N_A}} \qquad (7)$$

where ρ is the specific weight of the protein and N_A is the Avogadro number. For TMR-labeled hRepA, the diffusion time τ_{diff} can be calculated according to eqs 3−5 assuming a molecular weight of 200 000 and a lateral axial distance r_0 for the observation volumes of 0.24 μm (*17*). The calculated value for the diffusion time τ_{diff} of such a ~200 000 mass protein is 0.289 ms (*17*). The measured diffusion time for TMR-labeled hRepA in buffer at pH 8.0, 0.32 ± 0.03 ms, agrees within the error range with this value, while the diffusion times for the complexes with ssDNA in buffer at pH 5.8 are significantly longer (see Table 1). The shorter diffusion times of the hexameric TMR-hRepA compared with the longer diffusion times of the ssDNA/hRepA complexes indicate that dimeric hRepA molecules are bound to one or several BFL-ssDNAs in these complexes.

Attempts to follow the kinetics of complex formation by FCS between BFL-ssDNA and hRepA under pseudo-first-order conditions with respect to BFL-ssDNA were not successful. Complex formation was so fast that after mixing of ssDNA and hRepA, the reaction was completed before the first autocorrelation function could be recorded within 10−20 s. Therefore, it is necessary to apply fast reaction methodology like stopped flow or temperature jump to investigate the kinetics of ssDNA binding to hRepA.

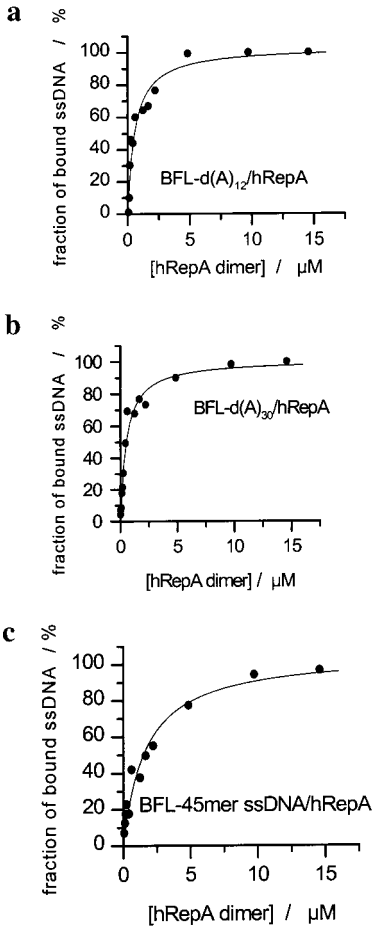

FIGURE 2: Equilibrium binding of BFL-d(A)$_{12}$ (a), BFL-d(A)$_{30}$ (b), and BFL-45mer ssDNA (c) to hRepA dimer at pH 5.8. BFL-ssDNA concentration was 15 nM in each case ([ATPγS] = 0.5 mM). The relative fraction of complex formed (z) is plotted against the hRepA dimer concentration. Nonlinear fits yield the apparent dissociation constants of the different ssDNA/hRepA dimer complexes with values of 0.58 ± 0.12 μM (a), 0.52 ± 0.07 μM (b), and 1.66 ± 0.32 μM (c).

(B) Determination of the Dissociation Constants. Figure 2a−c shows the binding curves for the titration of three different BFL-labeled single-stranded oligodeoxynucleotides with increasing concentrations of hRepA dimer in the presence of 0.5 mM ATPγS at pH 5.8 and 25 °C. For the determination of apparent dissociation constants, the fraction of bound ligand, z, was measured at a constant concentration of BFL-ssDNA as a function of the concentration of hRepA dimer. The fraction of bound ligand (BFL-ssDNA/hRepA dimer) was plotted against the hRepA dimer concentration, and the data were described by a nonlinear regression model according to eq 8 for the binding of BFL-ssDNA to one binding site present on hRepA dimer as shown by additional ultracentrifugation experiments (*13*):

$$z = F\frac{[\text{hRepA dimer}]}{[\text{hRepA dimer}] + K_{d(app)}} \qquad (8)$$

F denotes the fraction of bound ssDNA at infinite hRepA dimer concentration and $K_{d(app)}$ the apparent dissociation

Table 2: Apparent Hydrodynamic Radii (R_h) and Diffusion Coefficients (D) for hRepA and Aggregates As Determined by PCS[a]

pH		R_h (nm) of hRepA	D (m^2/s)	R_h (nm) of hRepA aggregates	D (m^2/s)
8.0	TMR-hRepA	5.9 ± 0.4	$(3.7 \pm 0.25) \times 10^{-11}$	–	–
7.6		6.3 ± 0.5	$(3.5 \pm 0.3) \times 10^{-11}$	–	–
6.5		6.5 ± 0.6	$(3.4 \pm 0.3) \times 10^{-11}$	–	–
5.8		7 ± 0.5	$(3.1 \pm 0.2) \times 10^{-11}$	77 ± 15, 152 ± 30	$(2.8 \pm 0.6) \times 10^{-12}$, $(1.4 \pm 0.3) \times 10^{-12}$
5.8	+ATPγS, +ssDNA	8.4 ± 0.8	$(2.6 \pm 0.3) \times 10^{-11}$	58 ± 11, 114 ± 23	$(3.8 \pm 0.8) \times 10^{-12}$, $(1.9 \pm 0.4) \times 10^{-12}$

[a] The apparent hydrodynamic radii (R_h) were calculated from the measured diffusion coefficients (D) according to eq 4. Experimental conditions: PCS measurements at neutral pH were performed with 40 mM Tris-HCl buffer at pH 7.6 or 40 mM MES−NaOH buffer at pH 6.5. TMR-hRepA was measured in 20 mM Tris-HCl buffer at pH 8.0. Under acidic pH conditions, 40 mM MES−NaOH buffer at pH 5.8 (10 mM $MgCl_2$) was used. For PCS experiments in the presence of ssDNA, 10 μM $d(A)_{30}$ and 100 μM ATPγS were included in a 40 mM MES−NaOH buffer of pH 5.8 (10 mM $MgCl_2$). hRepA concentration: 0.15 mg/mL (0.83 μM). (−) Aggregates of hRepA could not be detected.

constant of the 1:1 complex. For each protein concentration, the fraction of dimer and aggregated protein was determined by ultracentrifugation (data not shown). Finally, the dimer concentration was used for the calculation of the dissociation constants according to eq 8.

The data obtained with the ultracentrifuge are consistent with the binding of BFL-ssDNA to one site on the hRepA dimer with no indication of cooperativity since the binding curves are not sigmoidal. For the apparent dissociation constants, $K_{d(app)}$, of complexes between hRepA dimer and BFL-labeled $d(A)_{12}$, $d(A)_{30}$, and 45mer ssDNA (for the sequence, see Experimental Procedures), values of 0.58 ± 0.12, 0.52 ± 0.07, and 1.66 ± 0.32 μM were obtained in FCS experiments at pH 5.8 and 25 °C in the absence of NaCl with 0.5 mM ATPγS and 10 mM $MgCl_2$. Without ATPγS (pH 5.8), only 7% of complex was formed between 15 nM BFL-$d(A)_{30}$ and 40 μM hRepA. At pH 7.6 (with ATPγS), only 18.4% complex formation was observed even in the presence of more than 2000-fold excess of hRepA with respect to BFL-ssDNA while at pH 5.8 (with 0.5 mM ATPγS) the formation of complex was determined to be 100% for all three ssDNA molecules at such a [hRepA]:[ssDNA] ratio (Figure 2a−c). If ATPγS was replaced by 0.5 mM ADP at pH 5.8, only 9.3% of complex was formed even in the presence of more than 2000-fold excess of hRepA with respect to BFL-ssDNA. The affinity of hRepA for BFL-labeled single-stranded oligodeoxynucleotides in the absence of a stable ATP analogue, like ATPγS, or in the presence of ADP as nucleotide cofactor and at neutral pH was too low to enable measurements of equilibrium binding curves by FCS. Under these conditions, $K_{d(app)}$ was estimated to lie in the range between 10 and 250 μM.

Photo Correlation Spectroscopy (PCS) Studies. The apparent hydrodynamic radii (R_h) and the diffusion coefficients (D) of the complexes of hRepA dimer with ssDNAs were also measured in PCS experiments and are comparable to those derived by FCS (Tables 1 and 2). In contrast to our FCS experiments, the apparent hydrodynamic radius of hRepA at pH 7.6 is practically the same as the R_h of hRepA and its complex with ssDNA detected in PCS experiments both in the absence and in the presence of ssDNA at pH 5.8 (Table 2). Due to aggregation, higher molecular weight components were observed besides hRepA dimer at pH 5.8. Despite this aggregation, no significant change of the apparent hydrodynamic radius of hRepA was observed in the presence of ssDNA at pH 5.8 (Table 2). These findings support the assumption that the complexes between BFL-ssDNA and hRepA detected by FCS at pH 5.8 consist of dimeric hRepA and one or several ssDNAs.

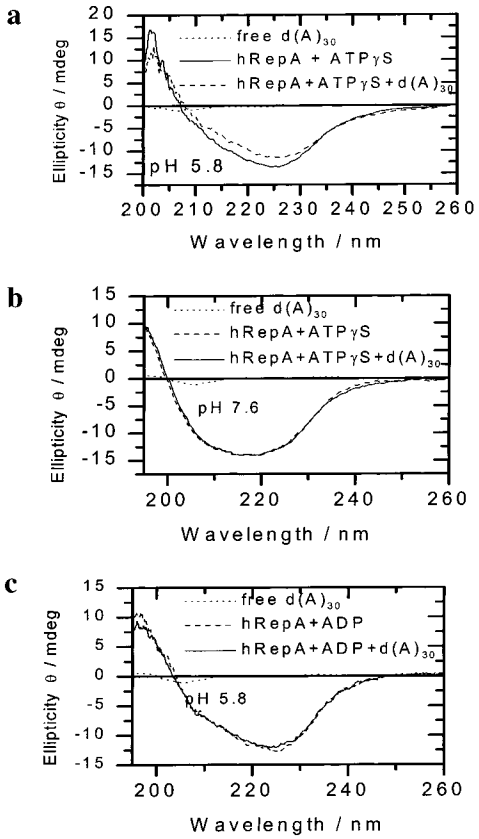

FIGURE 3: (a) CD spectra of 1.7 μM hRepA with 20 μM ATPγS as cofactor in the presence and absence of 1.7 μM $d(A)_{30}$ in 40 mM MES−NaOH (10 mM $MgCl_2$) at pH 5.8. (b) CD spectra of 1.7 μM hRepA with 20 μM ATPγS as cofactor in the presence and absence of 1.7 μM $d(A)_{30}$ in 40 mM Tris-HCl (10 mM $MgCl_2$) at pH 7.6. (c) CD spectra of 1.7 μM hRepA with 20 μM ADP as cofactor in the presence and absence of 1.7 μM $d(A)_{30}$ in 40 mM MES−NaOH (10 mM $MgCl_2$) at pH 5.8.

Isothermal Titration Calorimetry (ITC) Studies. ITC experiments at pH 5.8 yielded an exothermic enthalpy change ΔH_b of -3.2 ± 1.2 kJ/mol associated with the binding of $d(A)_{12}$ to hRepA, which was too small for measuring complete binding curves (data not shown). For this reason, it was not possible to determine the stoichiometry, n, and the apparent dissociation constant, $K_{d(app)}$, of the hRepA/ssDNA complexes independently by ITC.

Circular Dichroism Spectroscopy (CD) Studies. CD spectra of hRepA show an increase of the absolute ellipticity (θ) values between 235 and 210 nm only at pH 5.8 in the presence of ATPγS, probably due to a structural transition upon binding of ssDNA (Figure 3 a). This change does not occur at pH 7.6 and at pH 5.8 with ADP instead of ATPγS

(Figure 3b,c), in agreement with the relative affinities of hRepA for ssDNA under such conditions as observed in FCS experiments.

DISCUSSION

An understanding of helicase mechanisms requires studies of the interactions of helicase with its DNA substrate, especially the binding oligomeric states, binding stoichiometries, and binding affinities and the influence of nucleotide cofactors which will switch the energetics of protein or protein−DNA assembly and thus the distribution of assembly states.

Fluorescence correlation spectroscopy (FCS) is a powerful tool to examine molecular interactions as well as their time dependence. It has the advantage that the interaction can be analyzed rapidly in small volumes without the need for separating unbound from bound ligand. In this study, the mass difference between hRepA and the ssDNA fragments used is large enough to enable FCS measurements that distinguish between free BFL, labeled BFL-ssDNA, and the complex between ssDNA and hRepA in solution. The autocorrelation functions thus provide the fraction of labeled BFL-ssDNA bound to hRepA.

ssDNA Binding to hRepA Is Optimal at Acidic pH in the Presence of Nucleoside Triphosphate Which Is Also Optimal for Unwinding Reactions. Since hRepA unwinds dsDNA independent of sequence, its binding affinity to ssDNA should be low in comparison to proteins binding to specific DNA sequences, which is in agreement with the present studies. In the absence of a stable ATP analogue or at neutral pH, the affinity of hRepA for ssDNA is so low that it is impossible to measure binding curves by FCS. Under these conditions, the dissociation constant, $K_{d(app)}$, is in the range between 10 and 250 μM. This is consistent with analytical ultracentrifugation at pH 7.6 in the presence of 60 mM NaCl, which showed a dissociation constant of 25.4 ± 6.4 μM for $d(A)_{30}$ binding to hRepA (*13*). hRepA has a narrow pH optimum for the dsDNA unwinding reaction in a remarkably low pH range between pH 5.5 and pH 6.0 (*4*). As reported here, binding of ssDNA to hRepA is also optimal under these pH conditions.

CD spectra indicate a structural transition of hRepA upon ssDNA binding which was only observed in the presence of a stable ATP analogue at pH 5.8. At neutral pH and with ADP as nucleotide cofactor, no change in the CD spectra occurred in the presence of ssDNA.

High Salt Concentration Inhibits ssDNA Binding to hRepA Helicase. Analytical ultracentrifugation experiments showed the dissociation constant, $K_{d(app)}$, for the $d(A)_{30}$/hRepA dimer complexes at pH 5.8 in the presence of 60 mM NaCl to be 0.94 ± 0.13 μM (*13*). In contrast, in the absence of NaCl, $K_{d(app)}$ for the binding of $d(A)_{30}$ to hRepA dimer was determined to be 0.52 ± 0.07 μM by FCS. These findings show that NaCl at a concentration of 60 mM increases the apparent dissociation constant of the ssDNA/hRepA dimer complex, in agreement with the inhibitory effect of NaCl on the helicase reaction (*5*).

Dimers of Hexameric RepA Bind to BFL-Labeled DNA at Optimal Helicase Activity Conditions. In solution at pH 7.6, hRepA exists as a homohexamer of 180 kDa (*10*) but forms a dimer of 360 kDa at pH 5.8 (*13*). PCS experiments are not able to detect the difference in the hydrodynamic radii between hRepA at pH 7.6 and its dimer at pH 5.8 due to the small increase of the radius, *R*, of 26% upon dimer formation (Table 2). The X-ray structure of hRepA crystallized at pH 6.0 also shows that a dimer of two hexameric hRepA molecules occupies the asymmetric unit (*11*).

The coexistence of higher aggregates and hRepA dimer was demonstrated by PCS both in the absence and in the presence of ssDNA and ATPγS at pH 5.8. If aggregates of hRepA bind BFL-labeled ssDNA, then the diffusion times of the corresponding complexes should have been shifted to significantly higher values, which was not observed in our FCS experiments. From the present FCS and PCS measurements, we conclude that higher aggregates of hRepA do not bind ssDNA and therefore the hRepA dimer is the active ssDNA binding form at pH 5.8.

One ssDNA Binding Site on hRepA. Analytical ultracentrifugation experiments (*13*) showed that at pH 5.8 and 10 °C in the presence of 0.5 mM ATPγS and 60 mM NaCl the stoichiometry, *n*, for the $d(A)_{30}$/hRepA dimer complexes at pH 5.8 is 1:1 [one $d(A)_{30}$ molecule per hRepA dimer]. Using FCS, it was not possible, however, to discriminate between mono-, bi-, and multiliganded RepA. By contrast, the recently developed photon counting histogram analysis would allow determination of the number of labeled ssDNA molecules bound to hRepA (*32*). This method measures the brightness of separate fluctuations, rather than evaluating the autocorrelation function as done in normal FCS.

Figure 2a−c shows that the fraction of labeled BFL-ssDNA bound to hRepA dimer depends on the hRepA dimer concentration and is typical for binding of ssDNA to only one binding site present on hRepA dimer in the presence of ATPγS. A cooperative behavior of hRepA as reported for other helicases (*33, 34*) was not observed in the FCS experiments reported here since the binding curves displayed in Figure 2a−c are not sigmoidal.

Length of ssDNA Required for Optimal Binding to hRepA. Experiments of ssDNA-dependent ATP hydrolysis catalyzed by hRepA indicate that the minimum length of DNA for tight interaction with hRepA is $n = 10$ deoxynucleotides (*12*). For ssDNA with $n \leq 10$, the rates of ssDNA-dependent ATP hydrolysis decrease sharply whereas binding of longer ssDNA with $n \geq 10$ is not significantly enhanced compared with $d(A)_{10}$.

In the presence of ATPγS and $MgCl_2$ at pH 5.8 and 25 °C without NaCl, the FCS-measured affinity of hRepA dimer for a 12mer ssDNA is the same as for a 30mer ssDNA (0.58 ± 0.12 and 0.52 ± 0.07 μM); for 45mer ssDNA, a slightly higher apparent dissociation constant of 1.66 μM was determined, corresponding to a lower affinity of hRepA dimer for 45mer ssDNA compared with $d(A)_{12}$ and $d(A)_{30}$. This is probably due to the formation of a partial duplex structure of the 45mer ssDNA, which is likely to be stable even at room temperature (see Experimental Procedures) and may reduce the affinity of hRepA for the single-stranded part of 45mer ssDNA. $d(A)_n$ single-stranded oligodeoxynucleotides can also form duplex structures at pH 4.0 and below (*35*). Since FCS at pH 5.8 and 7.6 showed no difference between the diffusion times of BFL-$d(A)_{12}$ and BFL-$d(A)_{30}$ at both pH values, we conclude that both oligodeoxynucleotides are single-stranded at pH 5.8.

Characterization of ssDNA and hRepA Complex Formation. Based on the evaluation of the autocorrelation functions, a common mechanism for complex formation in solution could be derived.

The mean value of the apparent hydrodynamic radius (R_h) of 6.6 ± 1 nm for hRepA determined by FCS and PCS at pH 5.8 agrees well with the geometry of the overall structure of a hRepA dimer. A single hRepA molecule is best described by a cylinder with a radius of 5.5 nm and a height of 6 nm with a central channel of 1.7 nm diameter (*11*). ssDNA is assumed to bind to this central channel of hexameric helicases (*6*−*8*). If two hRepA molecules are arranged bottom-to-bottom as shown by the crystal structure, the overall structure is 11 nm × 12 nm, which is consistent with an apparent hydrodynamic radius of 6.6 ± 1 nm. Dimer formation of hRepA does not prevent ssDNA binding as shown by the FCS experiments presented here and additional analytical ultracentrifugation experiments (*13*), suggesting that ssDNA binds to the central channel of hexameric helicases. It is assumed that during the unwinding reaction only one ssDNA molecule passes through the central channel and the other ssDNA moves along the outside of the helicase. Jezewska et al. have proposed strong and weak ssDNA binding sites present on helicase DnaB which may be involved in the unwinding reaction (*8*). According to this model, the 5′-end of ssDNA binds strongly to a subsite within the channel, while the same ssDNA strand near the entry site of duplex DNA is only weakly bound. The 3′ ssDNA leaves helicase DnaB at the outside during the unwinding reaction. From our experiments, we do not know where the ssDNA binds, but we observe only a single ssDNA binding site for each hRepA dimer with back-to-back orientation of the two hRepA molecules. Therefore, we can exclude additional weak binding sites present on the hRepA dimer in the concentration range studied. The tight binding of the short oligonucleotide (12mer) to hRepA dimer indicates that the ssDNA occupies the central cavity of hRepA and interacts with only one subunit at any time rather than being wrapped around the perimeter of the hexameric ring as proposed for Rho protein (*36*). Detailed understanding of how DNA interacts with RepA must await additional structural information, especially on hexameric helicase complexed with DNA.

ACKNOWLEDGMENT

We thank Dr. J. Schüler for valuable discussions concerning the FCS experiments and H. Roscher for technical assistance.

REFERENCES

1. Matson, S. W., and Kaiser-Rogers, K. A. (1990) *Annu. Rev. Biochem. 59*, 289−329.
2. San Martin, M. C., Stamford, N. P. J., Dammerova, N., Dixon, N. E., and Carazo, J.-M. (1995) *J. Struct. Biol. 114*, 167−176.
3. Engelman, E. H., Yu, X., Wild, R., Hingorani, M. M., and Patel, S. S. (1995) *Proc. Natl. Acad. Sci. U.S.A. 92*, 3869−3873.
4. Gogol, E. P., Seifried, S. E., and von Hippel, P. H. (1991) *J. Mol. Biol. 221*, 1127−1138.
5. Scherzinger, E., Ziegelin, G., Bárcena, M., Carazo, J. M., Lurz, R., and Lanka, E. (1997) *J. Biol. Chem. 272*, 30228−30236.
6. Yu, X., Hingorani, M. M., Patel, S. S., and Engelman, E. H. (1996) *Nat. Struct. Biol. 3*, 740−743.
7. Jezewska, M. J., Rajendran, S., Bujalowska, D., and Bujalowski, W. (1998) *J. Biol. Chem. 273*, 10515−10529.
8. Jezewska, M. J., Rajendran, S., and Bujalowski, W. (1998) *J. Biol. Chem. 273*, 9058−9069.
9. Sung, P., Higgins, D., Prakash, L., and Prakash, S. (1988) *EMBO J. 7*, 3263−3269.
10. Röleke, D., Hoier, H., Bartsch, C., Umbach, P., Scherzinger, E., Lurz, R., and Saenger, W. (1997) *Acta Crystallogr. D53*, 213−216.
11. Niedenzu, T., Röleke, D., Bains, G., Scherzinger, E., and Saenger, W. (2001) *J. Mol. Biol. 306*, 479−487.
12. Xu, H., Frank, J., Niedenzu, T., and Saenger, W. (2000) *Biochemistry 39*, 12225−12233.
13. Xu, H., Frank, J., Holzwarth, J. F., Saenger, W., and Behlke, J. (2000) *FEBS Lett. 482*, 180−184.
14. Trier, U., Olah, Z., and Schäfer-Korting, M. (1999) *Pharmazie 54*, 263−267.
15. Meseth, U., Wohland, T., Rigler, R., and Vogel, H. (1999) *Biophys. J. 76*, 1619−1631.
16. Oliver, R. A. W. *HPLC of Macromolecules: A practical approach*, IRL Press, New York.
17. Evotec GmbH, Physikochemische Betrachtungen zur FCS-Analytik (1995).
18. Elson, E. L., and Magde, D. (1974) *Biopolymers 13*, 1−27.
19. Magde, D., Elson, E. L., and Webb, W. W. (1974) *Biopolymers 13*, 29−61.
20. Magde, D., Webb, W. W., and Elson, E. L. (1978) *Biopolymers 17*, 361−376.
21. Eigen, M., and Rigler, R. (1994) *Proc. Natl. Acad. Sci. U.S.A. 91*, 5740−5747.
22. Rigler, R. (1995) *J. Biotechnol. 41*, 177−186.
23. Rigler, R., Mets, Ü., Widengren, J., and Kask, P. (1993) *Eur. Biophys. J. 22*, 169−175.
24. Schüler, J., Frank, J., Trier, U., Schäfer-Korting, M., and Saenger, W. (1999) *Biochemistry 38*, 8402−8408.
25. Meyer-Almes, F. J., Wyzgoll, K., and Powell, M. J. (1998) *Biophys. Chem. 75*, 151−160.
26. Berne, B. J., and Pecora, R. (1974) *Dynamic light scattering*, Wiley, New York.
27. Schmitz, S. K. (1990) *An introduction to dynamic light scattering by macromolecules*, Academic Press, New York.
28. Brown, W. (1993) *Dynamic light scattering, the method and some applications*, Oxford Science Publications, London.
29. Provencher, S. W. (1982) *Comput. Phys. Commun. 27*, 213−227.
30. Provencher, S. W. (1982) *Comput. Phys. Commun. 27*, 229−242.
31. Wiseman, T., Willistone, S., Brandts, J. F., and Lin, L.-N. (1989) *Anal. Biochem. 179*, 131−137.
32. Chen, Y., Müller, J. D., So, P. T. C., and Gratton, E. (1999) *Biophys. J. 77*, 553−567.
33. Jezewska, M. J., Kim, U.-S., and Bujalowski, W. (1996) *Biochemistry 35*, 2129−2145.
34. Menetski, J. P., and Kowalczykowski, S. C. (1985) *J. Mol. Biol. 181*, 281−295.
35. Fresco, J. R. (1959) *J. Mol. Biol. 1*, 106−110.
36. McSwggen, J. A., Bear, D. G., and von Hippel, P. H. (1988) *J. Mol. Biol. 199*, 609−622.

BI001543O